Green and Applied Chemistry

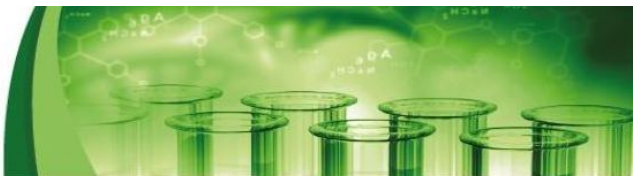

RHAZES: Green and Applied Chemistry

Vol. 14, 2022, pp. 95~115
ISSN: 2605-6895

CORROSION BEHAVIOUR OF WIRE PLUS ARC ADDITIVE MANUFACTURING (WAAM) BUILT HIGH STRENGTH PIPELINE STEELS

Najib Usman Shehu[a,b], Sue Impey[a] and Supriyo Ganguly[a]

[a] School of Aerospace, Transport and Manufacturing, Cranfield University, England, United Kingdom
[b] Department of Pure and Industrial Chemistry, Faculty of Physical Sciences, College of Natural and Pharmaceutical Sciences, Bayero University, Kano

Article Info

Article history:

Received 10/12/2021
Accepted 26/02/2022

Keyword:

ER90S-G,
Wrought,
Martensite,
Temper,
Corrosion

ABSTRACT

Wire and Arc Additive Manufacturing (WAAM) is of interest for many industries that requires parts with complex geometries via metal 3D printing. WAAM is capable of producing metal components with high deposition rates, large build volumes, minimum material waste and lead times and good structural integrity. Previous research in this field has focused on achieving correct geometrical and defect free deposition, while maintaining good mechanical properties when compared with wrought alloy. This is the first investigated study devoted to the corrosion behaviour of WAAM pipeline steels in artificial seawater. The corrosion rate of electrode rod 90 solid (ER90S-G) WAAM deposited low alloy steel (as deposited and heat-treated conditions) were compared to F22 wrought alloy of similar chemical composition. Corrosion behaviour of the low alloy steels were assessed using mass loss and electrochemical characterisation and correlated to the microstructural characteristics and hardness. The experimental results showed improved corrosion resistance and strength in ER90 WAAM built low alloy as compared to the wrought. Optical micrographs and hardness measurements confirmed that a martensitic structure was formed under air cooled condition in as deposited ER90, while tempered-martensitic structures were observed in heat treated ER90 and F22 wrought alloy steels. This research is the first step in creation of corrosion data of WAAM built structures and compare to their wrought version. This underpinning correlation between microstructural variation and corrosion pattern would allow modification of the WAAM process in a suitable manner for successful commercial applications.

Corresponding Author: Email: najman105@gmail.com

1. INTRODUCTION

Steel alloys are greatly important as engineering construction materials with substantial applications in numerous industries. Their widespread used is due to relatively economical extraction, refining, alloying, fabrication techniques, and versatility [Wan Nik *et al*., 2011]. Corrosion studies of steel alloys is of technical, economical, environmental and aesthetical importance. This is because corrosion transmute the properties of steel alloys thereby degrading the alloys and stimulating problems to oil and gas industries, particularly pipelines in marine environments [Goyal *et al*., 2018]. According to National Association of Corrosion Engineers (NACE) in 1998 and 2002, developed countries loss around 3.1 and 5.0% of their total Gross National Product (GNP) due to corrosion [Verma *et al*., 2017]. Steel alloys contribute significantly to these figures due to their magnificent physical and mechanical properties that makes them an important construction material for diverse industrial applications [Verma *et al*., 2016].

Availability of numerous steel types of similar chemical compositions but different mechanical properties, as well as increase in steel demand for engineering constructions oblige manufacturing industries to design and fabricate different steels for different applications. Thus, selecting the material that has the precise combination of characteristics for a distinct application is often a major concern [Callister, 2007].

Various elements have been used in alloying steel so as to improve its properties for different industrial applications. For corrosion scientists and materials engineers, variation in alloying elements alters the behaviour and properties of steels during application [Liu *et al*., 2019]. Molybdenum (Mo) has been a standard alloying element used in steel production, to lower creep rate and decelerates the coagulation and coarsening of carbides at high temperature application (e.g. power generation) [Masteel, 2017]. However, continuously addition of Mo to further improve its properties failed due to decrease in creep ductility and breaking down of cementite (Fe_3C) occurs at 500^{o}C [John, 2013]. A solution was found by incorporating Cr which offers many advantages not found in Mo-based alloys, hence, Cr-Mo steels were the first to allow steam temperatures on power stations to exceed 500^{o}C [Zima, 1977]. The additional strength and further corrosion resistance means that Cr-Mo alloys are supreme for industrial applications that operates equipment at elevated temperature environments beyond that of low carbon and Mo-based steels [Masteel, 2017].

Low alloy steel (e.g. F22 grade) manufactured using conventional hot forging has been used by oil and gas industries for pressure containing applications such as pipework and valve bodies. This is due to their chemical compositions, good weldability and other mechanical properties that makes them suitable for pipeline applications. The major drawbacks of the hot forging technique include; comparatively expensive tooling, defects produced by the processes or by post-process operations such as poor surface finish and warping while cooling, High temperature range (850-1150^{o}C for carbon and low alloy) which affects lubrication, and occurrence of oxidation and scaling on the workpiece [Rathi and Jakhade, 2014]. Wire plus arc additive manufacturing (WAAM) produces parts via metal 3D printing. This technique was developed to minimise the aforementioned problems associated with the conventional forging techniques.

WAAM has been evolved for the fabrication of high value materials for distinct application. Gas metal arc welding (GMAW) is a process in which a continuous solid wire (consumable electrode) is fed through the welding gun as feedstock material and electric arc is used as heat source. The movement of the deposition route in a layer-by-layer fashion to build the parts is controlled by a pre-programmed robot arm [Xu, *et al*., 2018]. WAAM is of interest for many industries because it produces parts with complex

geometries at high deposition rates, large build volumes, minimum material waste and lead times, and good structural integrity. These make WAAM an appropriate and possible technique for substituting the current means of manufacturing from forgings. Depositing >10 kg in steel and other metal alloys is possible using WAAM [Williams *et al*., 2016].
Electrode rod 90 solid (ER90S-G) and ASTM A182 F22 are low alloy steels, manufactured using GMAW and forging processes respectively with similar chemical compositions. A lot of work have been done to make the WAAM (ER90) wall similar to the wrought alloy (F22), and both steels are termed Chrome/moly (Cr-Mo) alloys with the former contained slightly higher chromium contents than the latter. Cr-Mo alloys are high-strength low alloy steels with excellent all-position welding performance. They are designed to intensify the substantial atmospheric corrosion resistance in marine environment. This research will help engineers assessing suitability of WAAM as a manufacturing technique for pipeline applications.
Several researches have been carried out on the corrosion and corrosion inhibition of mild steels in different media. However, there is no report to our knowledge on the corrosion behaviour of ER90S-G (as deposited and heat treated) and ASTM A182 F22 (quenched and tempered) in aerated and deaerated artificial seawater environments at room and elevated temperatures. Therefore, this investigation will explore the corrosion behaviour of WAAM deposited 2.4Cr 1Mo steel post heat treatment and to compare this with corrosion behaviour of wrought alloy steel of similar chemical composition manufactured using conventional forging. Mass loss and Linear Polarisation Resistance (LPR) techniques were employed. It is within the scope of this research to link the microstructural characteristics and strength of the low alloys using the optical microscope and hardness test measurements respectively.

2. MATERIALS AND METHODS

Block samples of WAAM built ER90S-G was produced by Cranfield University Welding Engineering and Laser Processing Centre while ASTM A182 F22 grade steels was purchased quenched and tempered, to be equivalent to the heat treated ER90. Samples were cut into coupons, each of dimensions 40 × 17 × 9mm. The coupons were labelled before grinding and polishing the surfaces with silicon carbide (SiC) abrasive (120 to 2500 grit). Each coupon was washed with distilled water, rinsed with isopropanol to remove residual water, fast dried to avoid premature corrosion and preserved. The compositional range of the steel samples were shown in Table 2.1 [AMS Special Metals; Lincoln, 2015].

Table 1: *Compositional Ranges of the Steels Samples Used*

Elements	ASTM A182 F22	ER90S-G
%C	0.08-0.15	0.06-0.12
%Cr	2.00-2.50	2.30-2.70
%Mo	0.90-1.10	0.90-1.10
%Mn	0.30-0.60	0.80-1.20
%Si	0.15-0.50	0.50-0.80
%P	0.025 max	0.02 max
%S	0.025 max	0.02 max
%Ni	0.50 max	< 0.10
%Cu	-	0.40 max
%Fe	Reminder	Reminder

These values conform to API 6A, PSL 3 requirements. A test solution was prepared by dissolving 35g NaCl in 635g deionised water to give 3.5% NaCl to represent brine. The same concentration was used throughout the project.

3. EXPERIMENTAL METHODS

3.1. Mass loss measurements

Low alloy (ER90 and F22) samples (40×17×9) mm were weighed for the original weight (W_o), and immersed in 130 mL of 3.5% NaCl solution. Contact was allowed for 24h in an open system at room temperature. The samples were withdrawn after a day, washed, rinsed in isopropanol, dried, reweighed and recorded the mass loss. Each experiment was carried out for ten days. The mass measurements were performed on Mettler FA2004 electronic balance. From the mass loss data, corrosion rate (mm/year) was compute using Equation 2.1 [NACE, 2017]:

$$CR\ (mm/year) = \frac{K \times W}{A \times T \times D} \qquad (2.1)$$

Where W is the mass loss (g) ($W = w_1 - w_2$), after 24h, A is the area of the steel samples (cm^2), T is the immersion time (h), D is the density (gcm^{-3}) (7.85 for low alloy steels), and K is a constant (8.76×10^4 for mm/year) [ASTM, 1999].

3.2. Electrochemical measurements

The low alloy specimens for electrochemical experiments were of similar dimensions as mentioned above. The cell used is a conventional three-electrode cell, where the samples, each of specified surface area (cm^2) were the working electrode (WE), with a platinum (Pt) wire counter electrode (CE) and saturated calomel electrode (SCE) as reference electrode (RE). The three electrodes were connected to electrochemical measuring instrument (GillAC). The open circuit potential (OCP) of the samples provides their stabilisation potential at zero current. The OCP of low alloy steels were measured using the steel samples as WE and SCE to which all the potentials are referred as RE without passing current through the system.

Linear polarisation resistance (LPR) tests were performed by immersing the samples (WE) along with CE and RE in 150ml 3.5% NaCl in aerated and deaerated solutions at room and elevated temperatures. The samples were polarised between -10 to +10mV and -50 to +50mV, at the standard sweep rates of $10mVm^{-1}$. Aeration was achieved by using a small air pump and the temperature was maintained in a water bath (Clifton, unstirred bath). The results were analysed and the corrosion current (I_{corr}) which corresponds directly to the corrosion rate was calculated using Stern-Geary equation shown below [Wan Nik, *et al*., 2011]:

$$I_{corr} = \frac{B}{R_p} \qquad (2.2)$$

$$B = \frac{b_c \times b_a}{2.303(b_c + b_a)} \qquad (2.3)$$

$$R_p = \frac{\Delta E}{\Delta I} \qquad (2.4)$$

Where, I_{corr} is the corrosion current, B is Stern-Geary constant, R_p is polarisation resistance (slope, also called LPR failure), and b_a and b_c are anodic and cathodic Tafel slopes respectively.

3.3. Effects of Alloying Composition and Microstructure

Grain structure, grain size, effects of alloying elements, and surface morphology were investigated by examining the micrographs of low alloy (ER90 and F22) steels. The specimens were cut into 17×9 mm and each potted in a mould (30 mm) exposing the X-Y and Y-Z planes. The mould is filled with a mixture of 25g epoxy resin and 3g hardener and allowed to solidify for 24h. The specimens were ground using SiC abrasive (120 to 2500 grit), polished, and etched with 2% Nital to determine the grain structure and other parameters. Surfaces were examined before and after corrosion using LEICA Nikon Eclipse ME600 and DM 2700 M optical microscopes respectively, at different magnifications.

3.4 Hardness Measurements

Vickers hardness tests were performed at room temperature, with respect to ISO 6507-1:2005. Specimens were prepared as for microanalysis before hardness tests, using a Zwick Roell AUTO-C.A.M.S. ® Computer Assisted Microhardness System. This comprised a diamond indenter and a light load to produce indentation on the low alloy samples. Measurements of the indentation depth or area left by the diamond, were converting into the hardness. 100g and 500g loads were applied for 15secs, and a total of 12 indentations were selected at different spatial positions of each sample.

3.5 Effect of heat treatment

To establish the effect of low alloy WAAM deposited and heat-treated samples (ER90 and F22), the coupons were subjected to 3.5% NaCl deaerated and aerated solutions at room and elevated temperatures. Results were gathered at room temperature for both mass loss and LPR measurements, and separately at elevated temperature using a water bath at 65°C using LPR.

4. RESULTS AND DISCUSSION

Presentation of the findings from mass loss and electrochemical measurements, as well as the micro examination and hardness test in relation to the corrosion behaviour of WAAM built high strength steels are contained under the following headings:

4.1. Mass Loss Analysis

The corrosion behaviour of low alloy (F22 and ER90) steels was examined by immersing the samples in 3.5% NaCl deaerated open system at room temperature. Mass loss method was initially used to observe the corrosion of different spatial positions (top, middle, and bottom) of WAAM deposited low alloy (and also heat treated) to compare with wrought alloy steel of similar chemical composition manufactured using conventional forging.

The average mass loss profile of the low alloy (F22, ER90 HT, and ER90 AD) steels obtained by exposing different spatial positions of the samples to the corrosion environment was shown in Figure 1. Consequently, results of the corresponding corrosion rates calculated from the mass loss data was depicted in Figure 2. As seen from the figures, low alloy mass losses and corrosion rates increases linearly with increase in immersion time. It can be observed from Figure 2 that there is minor variation in the corrosion rate of low alloy samples at room temperature, with F22 and ER90 AD showing slightly higher

and lower corrosion rates respectively. A similar observation was made by some workers. Liu *et al*. (2019) for example, examined that the mass loss of forged low alloy steel increases in seawater with immersion period.

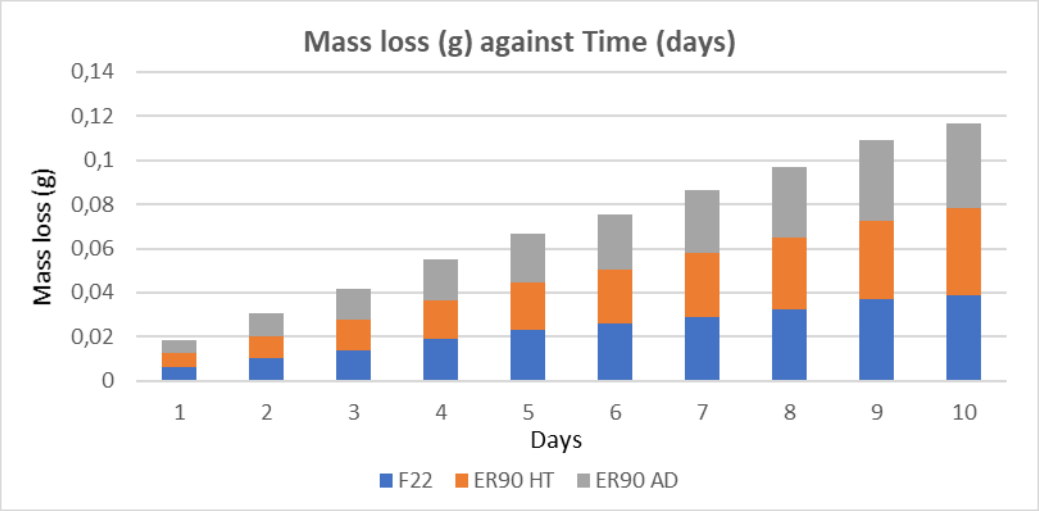

Figure 1: Variation of Mass Loss with Time for the Corrosion of Low Alloy (F22 and ER90) Steels in 3.5% NaCl Deaerated Open System at Room Temperature.

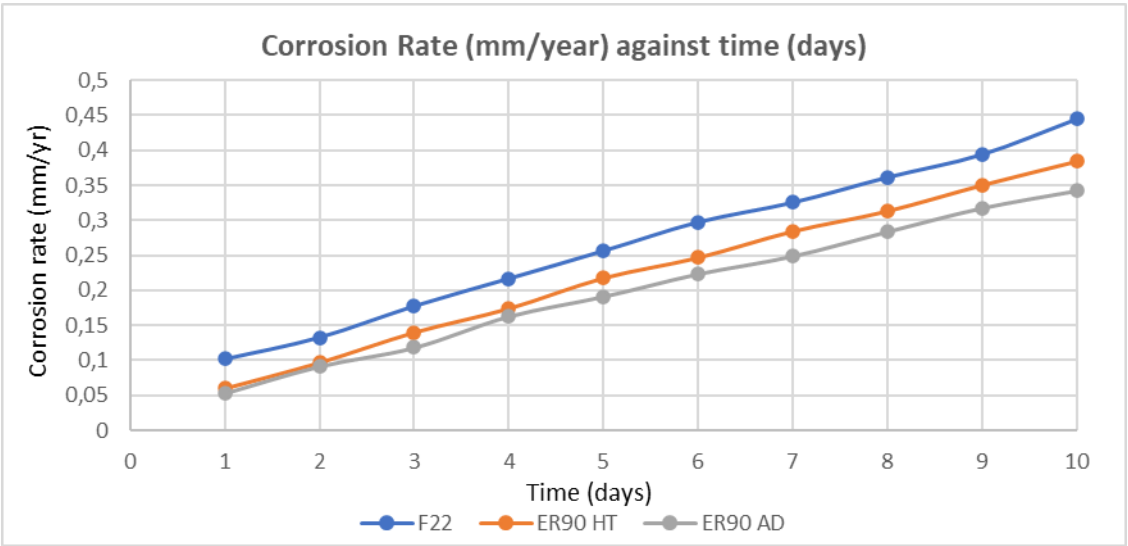

Figure 2: Variation of Corrosion Rates with Time for the Corrosion of Low Alloy (F22 and ER90) Steels in 3.5% NaCl Deaerated Open System at Room Temperature.

4.2. Electrochemical Profiling

The electrochemical measurements (OCP and LPR) of the low alloy (F22 and ER90) steel samples were checked to monitor the corrosion rates, establish corrosion rate in service with high sensitivity, assess rate controlling mechanism, and propose life prediction in some instances. This technique is faster and more reliable to researchers because it involves the use of a fast and accurate potentiostats, designed precisely for corrosion studies [Frankel, 2008]. The steel test samples were subjected to same environmental conditions mentioned above, and the first LPR was measured without settling and stabilising the samples in the media. This results in an undesirable and strange corrosion rate and potential results presented in Figures 3 and 4 respectively. It is unreasonable to take the average of these unreliable and immoderate results, and this prompt to settling and stabilising the samples by subjecting them to OCP in the media for a period of time before conducting another LPR measurement.

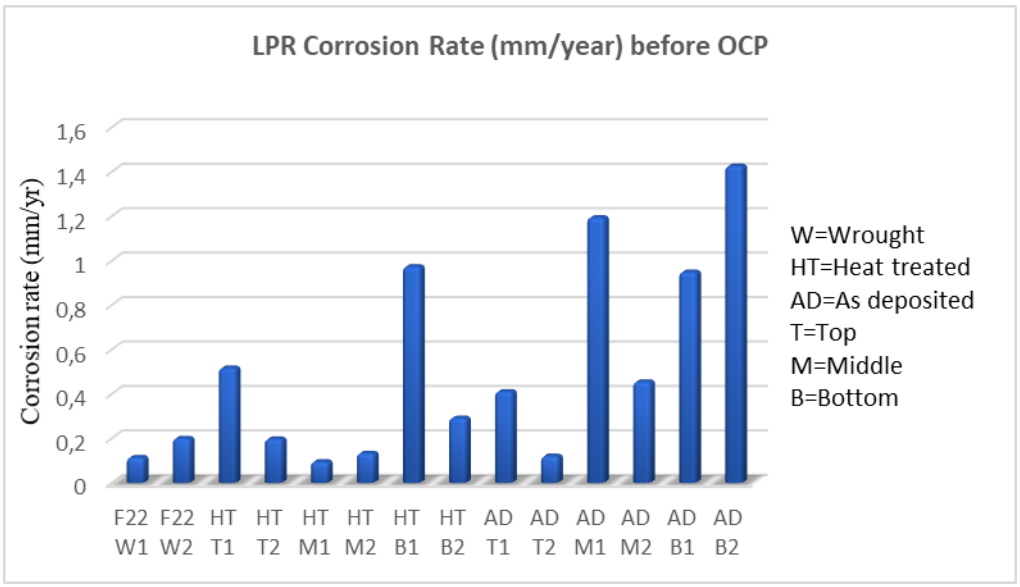

Figure 3: Corrosion Rate of Low Alloy (F22 and ER90) Steels in 3.5% NaCl Deaerated Solution at Room Temperature before Stabilisation.

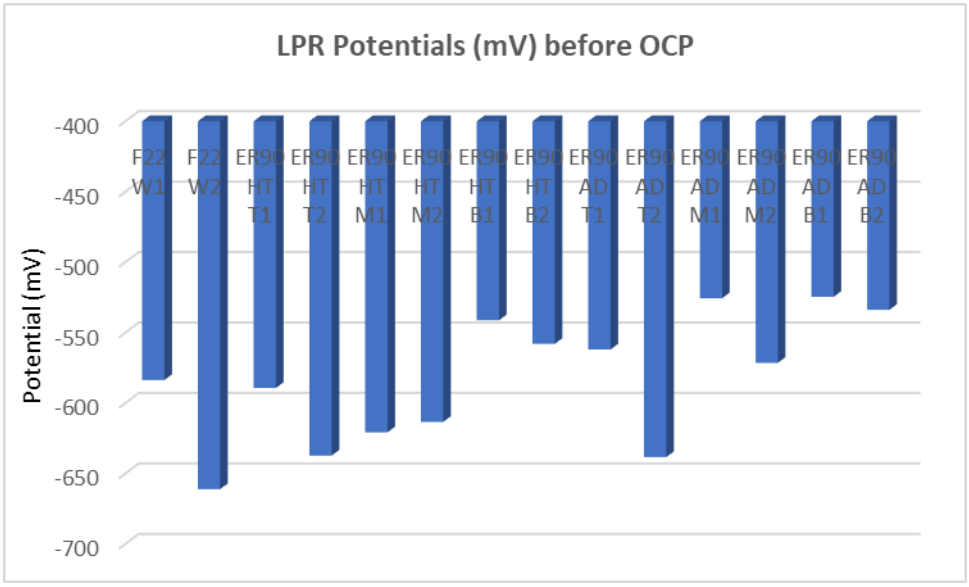

Figure 4: Potentials of Low Alloy (F22 and ER90) Steels in 3.5% NaCl Deaerated Solution at Room Temperature before Stabilisation.

The stabilisation potentials results obtained after settling the samples for 3000 seconds in 3.5% NaCl deaerated solution at room temperature was computed using OCP. The samples start settling at 1500 seconds and become more stable at 2500 seconds as depicted in the Figure. This indicates the settling and stabilising potential of each material exposed to this environmental condition. The stabilisation pattern shown in Figure 5 inferred that the low alloy steel samples settled at close range potentials.

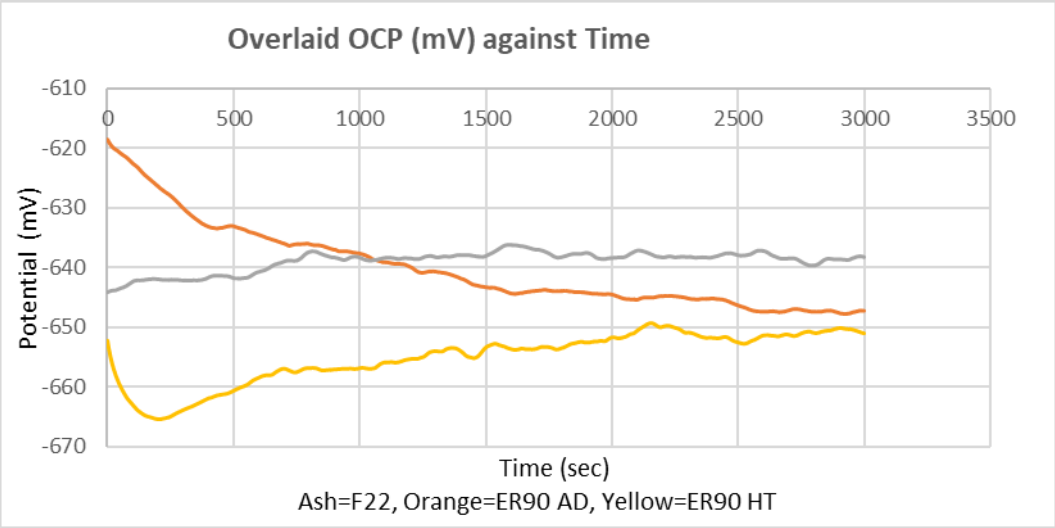

Figure 5: Overlaid Open Circuit Stabilisation Potentials (mV) of Low alloy (F22 and ER90) Steels in 3.5% NaCl Deaerated Solution at Room Temperature.

Conducting another LPR after stabilising the specimens in the media gives a more sensible and reasonable results. The average corrosion rates obtained from different spatial positions (T, M, and B), as well as the overall average of each sample (F22, ER90 HT and ER90 AD) were shown side by side in Figure 6. Their potentials were presented in Figure 7 as well.

It can be noticed from Figure 3.6 that the wrought alloy sample (F22) steel corrodes more than the low alloy (ER90 HT & AD) steels. This is due to the alloying compositions of both materials as shown in Table 2.1, which indicates that the low alloy WAAM deposit steels contained slightly higher chromium (Cr) content than the wrought alloy steel. This element plays a significant role in the corrosion resistance of low alloy steels [Lyon, 2010]. Similarly, the corrosion rates acquired by low alloy steels from LPR technique show similar trend as that of mass loss, with F22 and ER90 AD showing relatively higher and lower corrosion rates respectively. This slight variation could be due to the micro constituents of the low alloy (ER90) WAAM built deposit, which could be difficult to disrupt by the medium at room temperature. The average corrosion rates obtained from both LPR and mass loss in 3.5% NaCl deaerated solution at room temperature indicates that there is strong agreement between the results of the two methods.

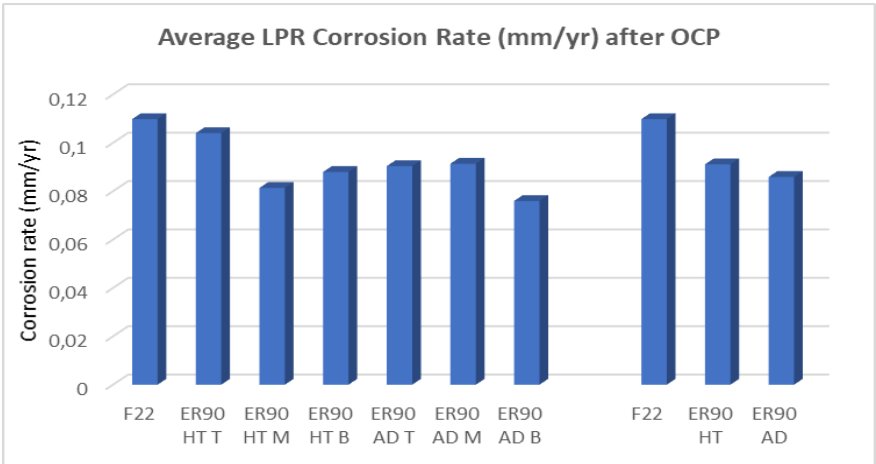

Figure 6: Corrosion Rate of Low Alloy (F22 and ER90) Steels in 3.5% NaCl Deaerated at Room Temperature after Stabilisation.

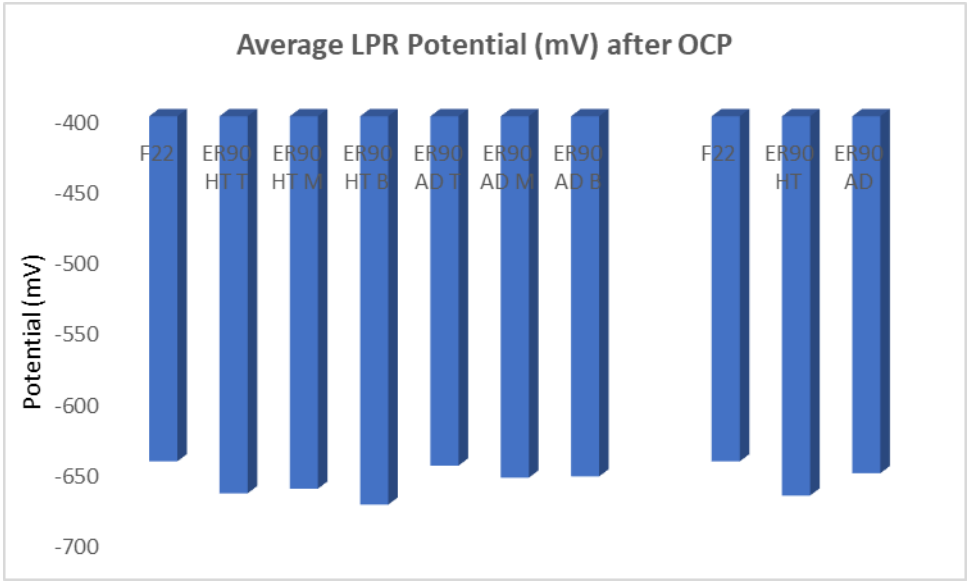

Figure 7: Average LPR Potentials of Low Alloy (F22 and ER90) Steels in 3.5% NaCl Deaerated Solution at Room Temperature after Stabilisation.

The results obtained at room temperature were in static and deaerated conditions, and low alloy (ER90 HT & AD) steels exhibit nearly similar performances in 3.5% NaCl solution at these conditions. But there is further needs to test other environmental parameters that might be in contact with the samples as the materials would likely to experience other factors while in service. These factors include; flowing, aeration, elevated temperature and others. As a results of these, both low alloy (F22 and ER90) steels samples were subjected to 3.5% NaCl aerated solution at elevated temperature of 65ºC for 1h. Bubbling air into the environment agitate the system continuously, and this covers the shaking factor. The average corrosion rate of the samples obtained using LPR at these conditions were shown in Figure 8, whereas their corresponding average potentials are in Figure 9.

Generally, elevating the temperature from room temperature to 65ºC causes the average corrosion rates of the low alloy steels to increase. A similar observation was made by Wan Nik *et al*. (2011), who reported that little rises in temperature affects the increasing in corrosion rate. Although the average corrosion rates of both samples increase at elevated temperature, WAAM build low alloy steels exhibit better corrosion resistance than the F22 wrought version, with ER90 HT and ER90 AD show virtually similar corrosion rate as presented in Figure 8.

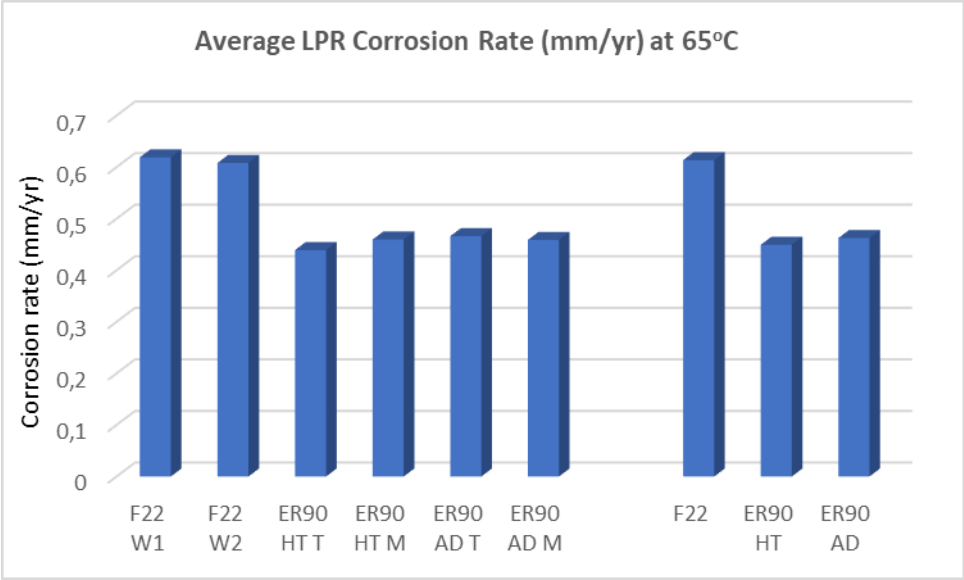

Figure 8: Average LPR Corrosion Rate of Low Alloy (F22 and ER90) Steels in 3.5% NaCl Aerated Medium at Elevated Temperature.

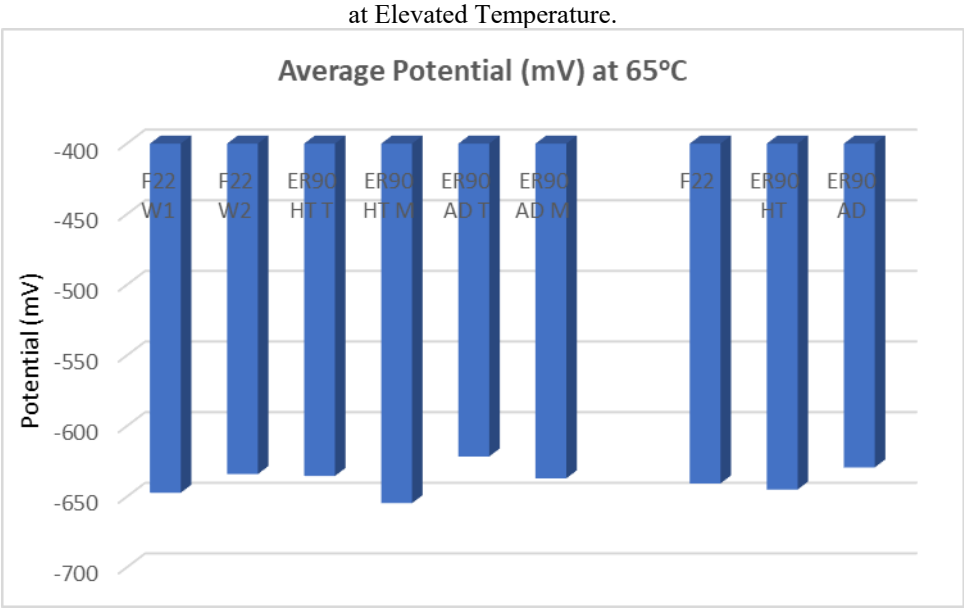

Figure 9: Average Potentials of Low Alloy (F22 and ER90) Steels in 3.5% NaCl Aerated Medium at Elevated Temperature.

It can be deduced from Figure 8 that the ER90 WAAM deposit (also heat treated) low alloy steel distinctly showed improved corrosion resistance, when compare with wrought alloy of similar chemical composition (Table 1). The average corrosion rates were in the following decreasing order (ER90 HT < ER90 AD < F22). The capability of ER90 WAAM as deposit and heat-treated samples to intensify the atmospheric corrosion resistance in aerated medium at 65°C was due to slightly higher chromium content in comparison with F22 wrought.

4.3 Effects of Alloying Composition, Microstructure and Hardness

Alloying constituents plays a significant effect on the corrosion behaviour as well as the microstructure of the material. The micro examination carried out on the X-Z and Y-Z planes of low alloy steels were shown in Figures 3.10-3.12 whereas the percentage compositions were listed in Table 1. Microstructural analysis of the steel materials was made to observe the effects in variation of alloy elements on the microstructure, and

correlate with the corrosion resistance performance. Carbon has a significant effect on both microstructure and hardness of the low alloy steels. Increasing carbon content generally improves the material strength. However, it reduces ductility, weldability, and martensite start temperature [Lyon, 2010].

Figure 10 (i)-(iv) are similar and shows a tempered martensite microstructure of F22 (i & ii) and heat treated ER90 (iii & iv) with uniformly dispersed compositions and very fine particles. These fine particles are due to the presence of carbide formers (Cr and Mo). Cr forms a hard and wear resistance carbide (chromium carbide) which increases corrosion and oxidation resistance, while Mo formed a carbide which produces fine grain and improves hardenability and reduce temper embrittlement [Callister and Rethwisch, 2011]. This compositional homogeneity is because the wrought alloy manufactured from hot forging was then quenched and tempered, while the WAAM deposit that process using thermo-mechanical controlled process, was also heat treated.

Figure 10 (v) and (vi) contain a martensitic structure (with needle shape grains) and a trace mixture of bainite, due to the presence of Cr, Mo, and Mn compositions. These compositions acquire the substitutional or interstitial position in the atomic site (depending upon the compositional size) which prevents diffusion and improve hardenability. Presence of Cr (2.40) and Mo (1.00) in appreciable quantity promotes nucleation and growth of non-equilibrium hard phases, which helps shifting the continuous cooling transformation (CCT) curve to the right. This will make it easier to achieve a martensitic and bainite microstructures, which increase hardenability [Callister, 2007].

Figures 11 and 12 indicates that the higher the Mo contents in a steel sample, the higher the hardness, while the higher the Cr contents the better the corrosion resistance. The order of Cr content in the low alloy steels was (ER90 > F22) in increasing order. Similarly, the order of hardness in the WAAM deposited (also heat treated) and wrought alloy samples was (ER90 AD > F22 > ER90 HT) in increasing hardness. Finally, the order of corrosion resistance was (ER90 > F22) in increasing resistance performance. This trend implies that the alloying elements and the microstructures greatly influenced the corrosion behaviour of the two steel samples in both aerated and deaerated as well as at room and elevated temperatures, where WAAM deposited low alloy steels shows improved corrosion resistance when compare with wrought low alloy version.

(i) X-Z Plane of F22 at x50

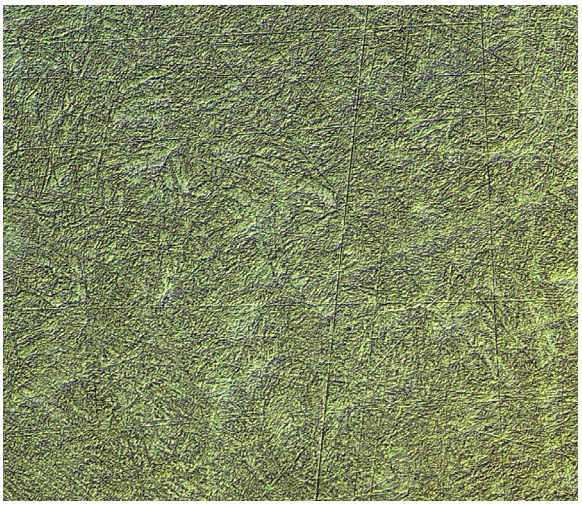

(ii) Y-Z Plane of F22 at x50

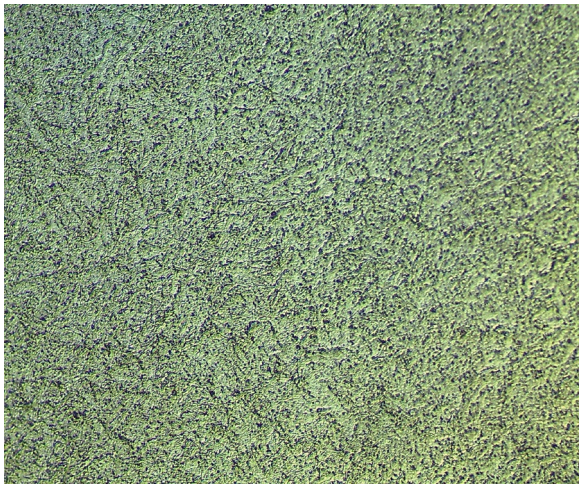

(iii) X-Z Plane of ER90 HT at x50

(iv) Y-Z Plane of ER90 HT at x50

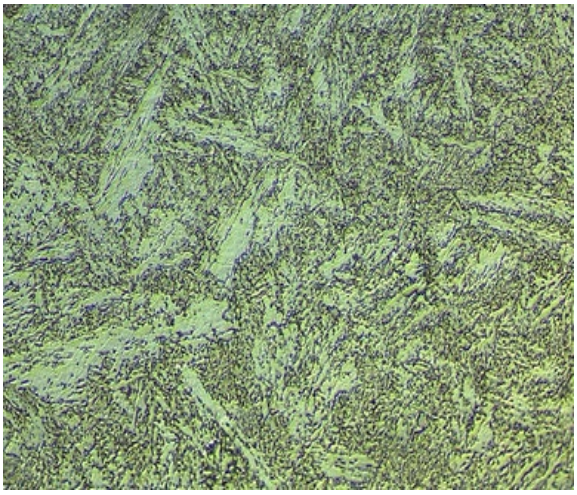

(v) X-Z Plane of ER90 AD at x50

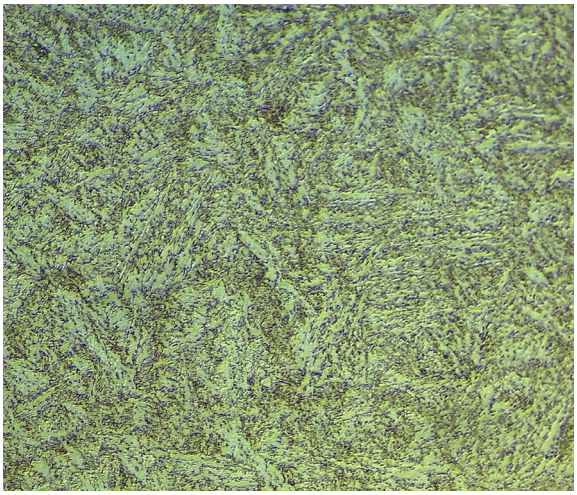

(vi) Y-Z Plane of ER90 AD at x50

Figure 10: Micrographs of Low Alloy (F22, ER90 HT and ER90 AD) Samples before Corrosion.

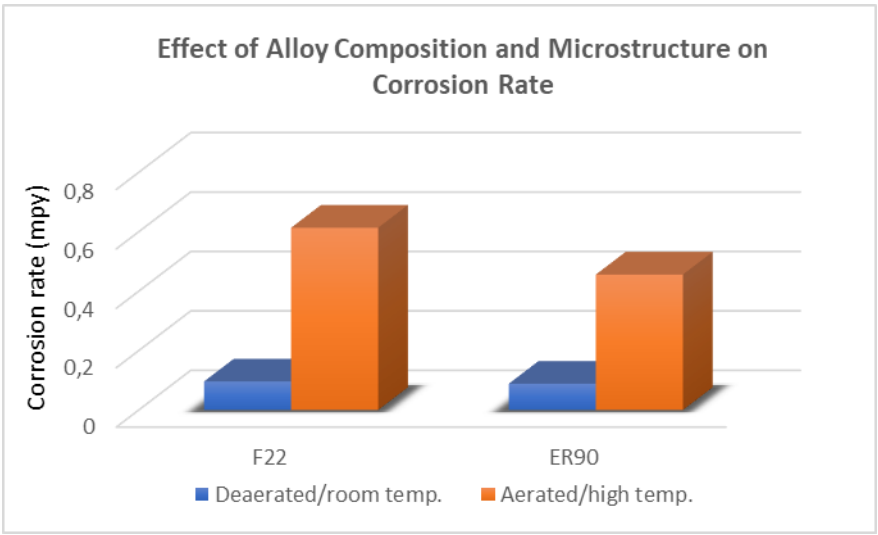

Figure 11: Effects of Composition and Microstructure on Corrosion Rate of ER90 WAAM Built and F22 Wrought Low Alloy Steels.

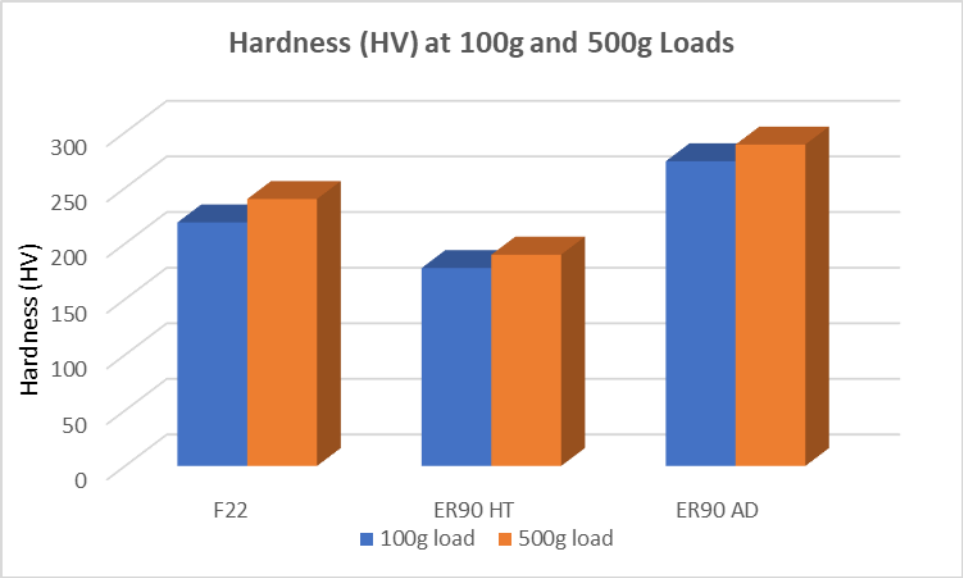

Figure 12: Average Hardness of Low Alloy (F22, ER90 HT and ER90 AD) Steel Samples.

4.4 Effects of Heat Treatment

Heat treatment is performed when certain properties were desired from a working sample such as grain refinement, uniformly dispersed composition, weldability, ductility, stress relieving, prevent micro-galvanic, and so on. In some instances, the heat treatment is accomplished without compromising other mechanical properties of the steel samples, while sometimes the reverse is the case. All these depends on the purpose of performing the heat treatment as well as the conditions at which the heat treatment was performed.

Martensitic ER90 WAAM low alloy deposit (Figure 10), (v) and (vi) is formed by heating the sample to its austenising temperature and rapidly quenched to relatively low temperature in oil or water to lock the carbon in its lattice (no diffusion). This was done in order to achieve desired microstructure (martensite), hardness and residual stress. The hardness is due to dissolved carbon in solid solution. Heat treatment of the ER90 WAAM deposit was performed in a furnace, where the quenched alloy steel was heated to a temperature (710^{o}C) where no phase transformation occurs (lower critical temperature) and hold for 1h, before cooling down at a controlled rate to temper the martensite at dwell time of 25^{o}C. This results in the heat treated ER90 low alloy steel (Figure 10), (iii) and (iv).

The corrosion behaviour of ER90 WAAM deposited low alloy (and also heat treated) was found to be nearly similar both at room temperature where ER90 AD (0.0859) shows slightly lower corrosion rate than ER90 HT (0.0911) and elevated temperature where ER90 HT (0.4495) shows slightly lower corrosion rate than ER90 AD (0.4626) as well (Figure 13). This indicates that the heat treatment has insignificant influence on the corrosion behaviour of ER90 AD and ER90 HT low alloys.

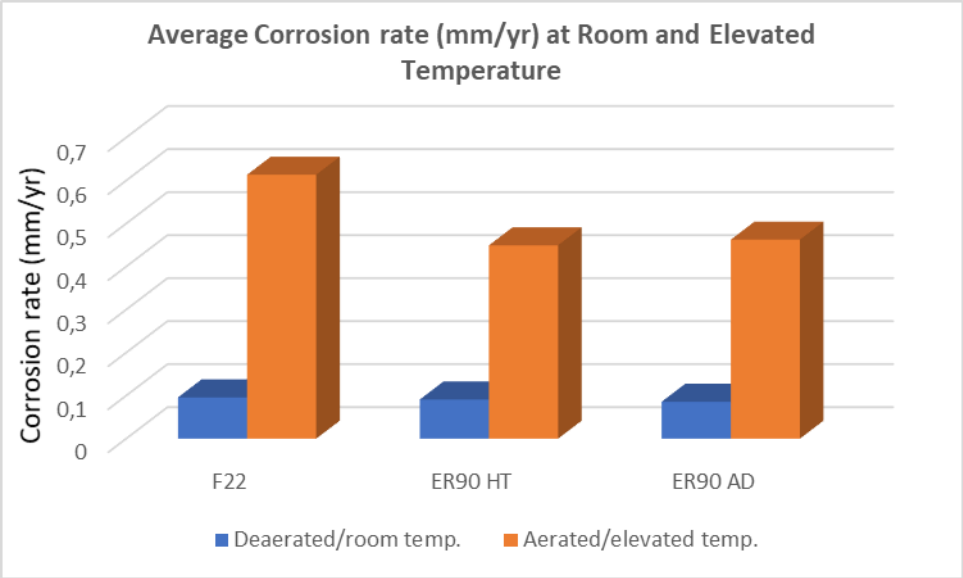

Figure 13: Average LPR Corrosion Rate of Low Alloy (F22 and ER90) Steels in 3.5% NaCl Aerated and Deaerated Media at Room and Elevated Temperatures.

4.5 Post Corrosion

Results of the corrosion products and patterns obtained after exposing the low alloy (F22 and ER90) steel samples into different environmental conditions were discussed here. Two sides of the X-Y plane of each corroded sample were displayed. Another phenomenon arouses after corroding the bottom samples of ER90 WAAM deposit low alloy steel was also analysed.

Figure 14 (i)-(vi) shows the corrosion pattern of low alloy steels after exposing into deaerated medium for 10 days, where (i) and (ii) represents F22 wrought alloy. Figure 14 (iii) & (iv) and (v) & (vi) illustrates heat treated and as deposited ER90 WAAM built alloy respectively. It can be seen from the figure that the wrought alloy (i) & (ii) deteriorate with a surficial roughness covering almost the entire surface of the sample due to contact with 3.5% NaCl. Conversely, heat treated ER90 low alloy sample (iii) & (iv) corrode in different fashion as that of wrought alloy, with its corrosion starts from the extreme edge of the sample, and increasing gradually as shown in Figure 3.14. ER90 WAAM deposited also show a similar pattern as the heat-treated counterpart as depicted in Figure 3.14 (iii) and (iv). This is due to variation in the Cr content (2.40 in ER90 WAAM and 2.25 in F22 wrought) in both samples where the WAAM alloy has 0.15 more compared to the wrought. This value greatly influenced the corrosion resistance of this material by forming a dispersed chromium carbide layer within the sample as the compositional effect of Cr was earlier discussed.

i) Side 1 X-Z Plane of F22

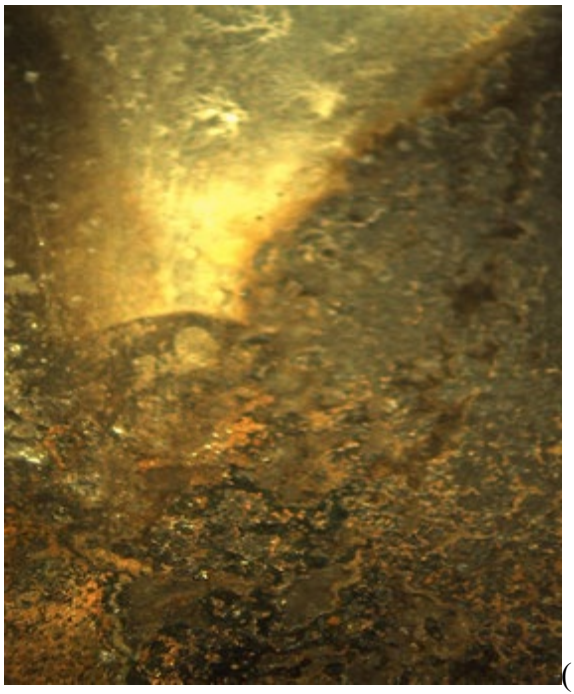

ii) Side 2 X-Z Plane of F22

iii) Side 1 X-Z Plane of ER90 HT

iv) Side 2 X-Z Plane of ER90 HT

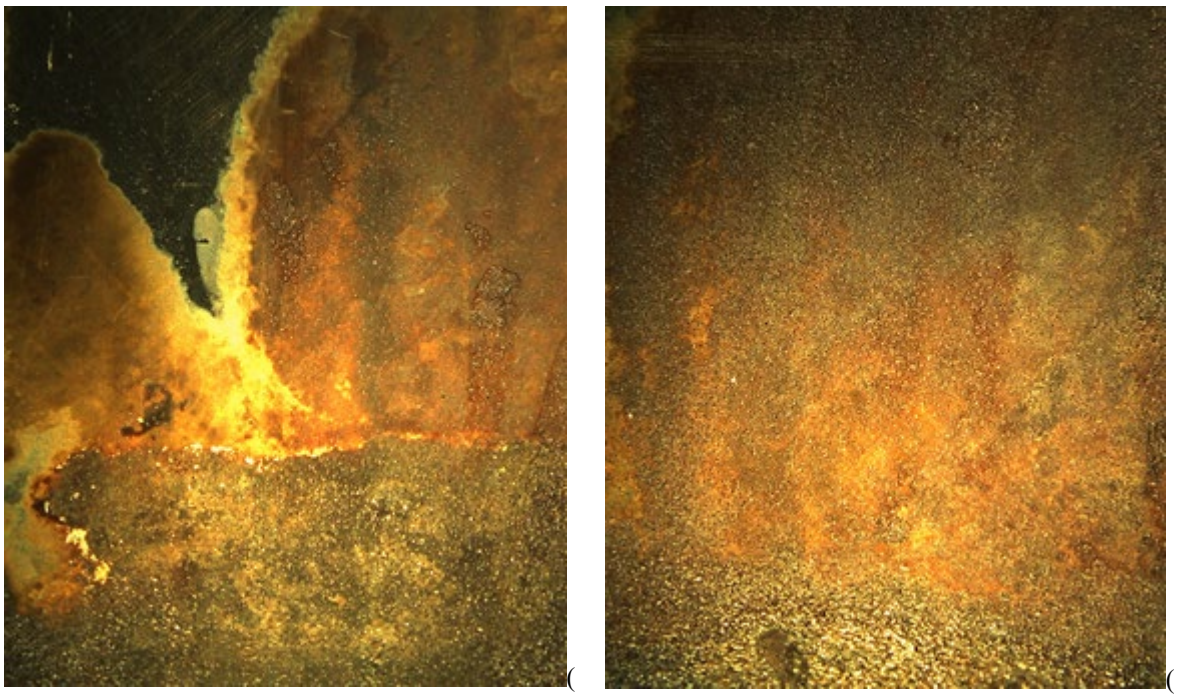

v) Side 1 X-Z Plane of ER90 AD vi) Side 2 X-Z Plane of ER90 AD

Figure 14: Micrographs for the Corrosion Behaviour of Low Alloy (F22 & ER90) Samples after 10 Days in 3.5% NaCl Deaerated Medium at Room Temperature.

Low alloy samples behave differently as mentioned above when subjected to 3.5% NaCl aerated solution at 65ºC. A rough texture can be seen in the surfaces of both low alloy samples as pictured in Figure 15. Wrought alloy (Figure 3.15), (i) & (ii) shows more surface roughness when compare to heat treated WAAM deposit low alloy (Figure 15), (iii) & (iv). A reddish-brown product appears clearly in side 1 of the wrought alloy, with some traces in side 2 (Figure 15), (i) & (ii). These products were not seen on the either side surface of the heat treated WAAM low alloy sample (Figure 15), (iii) & (iv). The reason still being the variation of Cr content in the two samples.

The surface roughness of as deposited ER90 low alloy steel appear a little different from that of heat treated, where some parts show more roughness than others with a trace of reddish-brown products on the topmost right of side 1 (Figure 15), (v) & (vi). This could be due to uneven distribution of Cr in the deposited sample which could results in accumulation of Cr on the part with less roughness and vice-versa. The part of the sample with reddish brown also indicates less Cr which could leads to micro-galvanic due to heterogeneous composition. This phenomenon was not observed in the heat-treated sample due to even dispersion of the Cr within the sample.

i) Side 1 X-Z Plane of F22

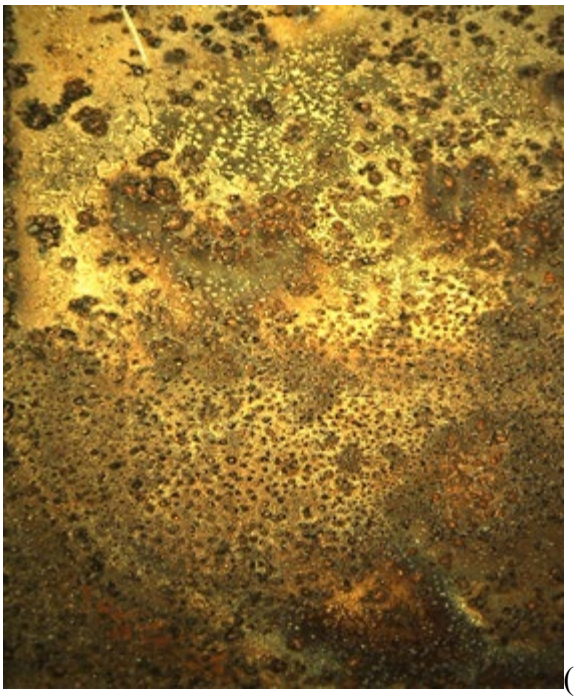

ii) Side 2 X-Z Plane of F22

(iii) Side 1 X-Z Plane of ER90 HT

iv) Side 2 X-Z Plane of ER90 HT

(v) Side 1 X-Z Plane of ER90 AD

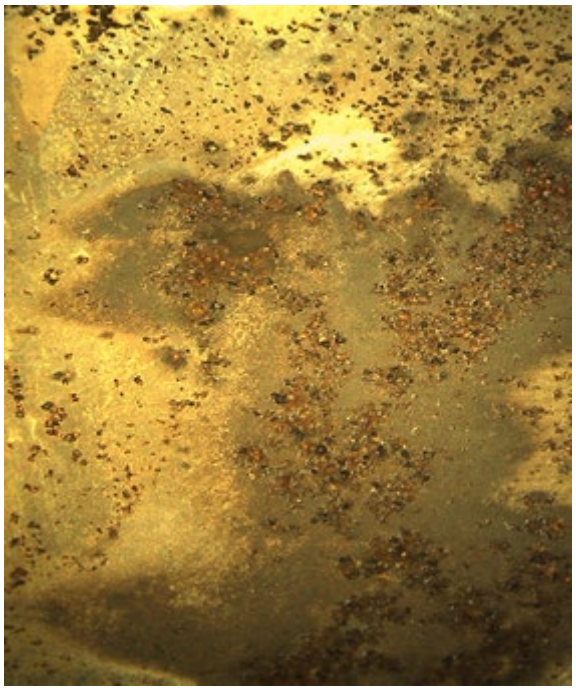

(vi) Side 2 X-Z Plane of ER90 AD

Figure 15: Micrographs for the Corrosion Behaviour of Low Alloy (F22, ER90 HT and ER90 AD) and Samples after 1h in 3.5% NaCl Aerated Medium at 65ºC.

The bottom samples of both as deposited and heat treated ER90 WAAM alloy shows a unique pattern after corroding in 3.5% NaCl deaerated solution for 10 days at room temperature (Figure 16), (i) & (ii). This enabled further investigation on why this occurred. One of the samples was ground, polished, etched (Figures 16), (iii) & (iv), and subjected to micro examination and hardness test. The microstructure (Figure 17) obtained shows that the two materials are apparently dissimilar. Correspondingly, different hardness values acquired from the two distinct sides support the microstructure, confirming that the top part is the WAAM built wall whereas the bottom part is the substrate (S375) on which the WAAM wall was built. This brought about a galvanic coupling with one of the materials (ER90 and/or S375) serve as cathodic and the other as anodic.

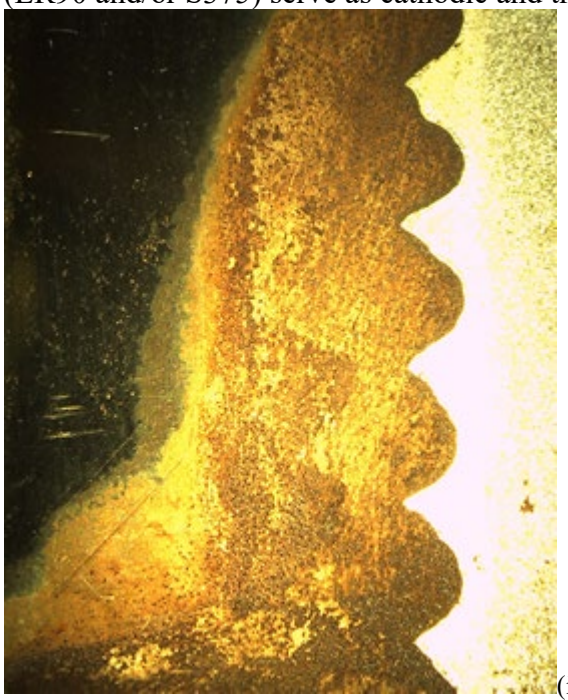

(i

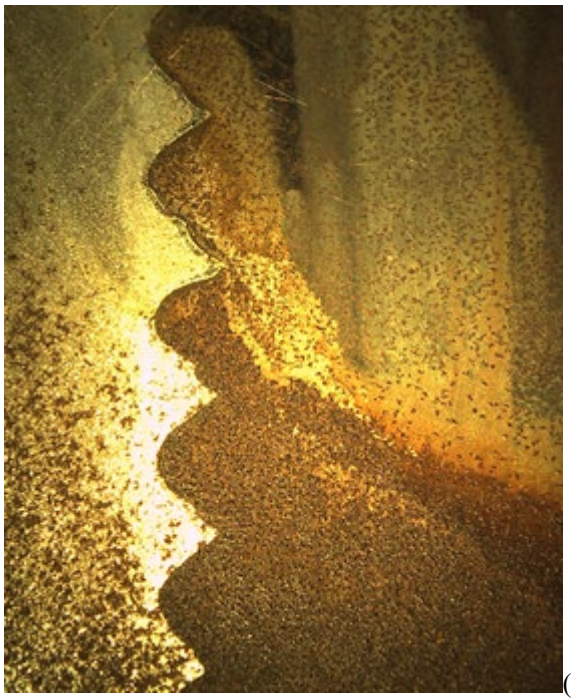

(

) Side 1 X-Z Plane of ER90 HT

ii) Side 2 X-Z Plane of ER90 HT

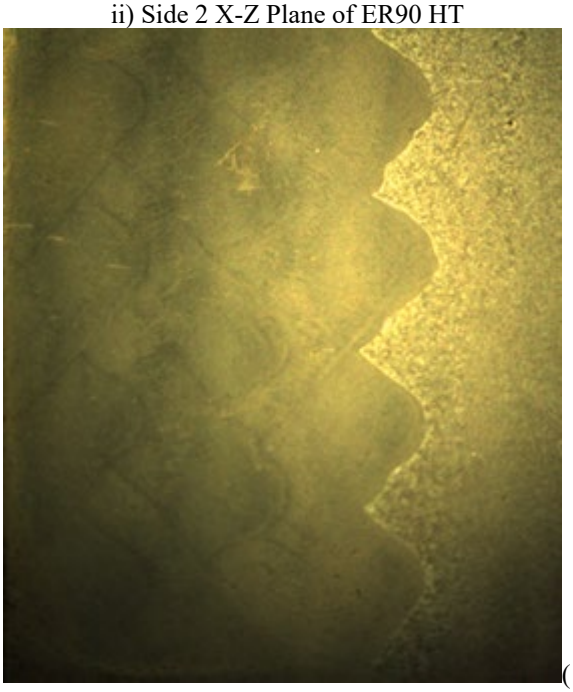

(i

(

ii) Side 1 X-Z Plane of Etched Bottom Sample

iv) Side 2 X-Z Plane of Etched Bottom Sample

Figure 16: Micrographs for the Corrosion Behaviour of Low Alloy (ER90 HT) Bottom Sample after 10 Days in NaCl Deaerated Solution at Room Temperature.

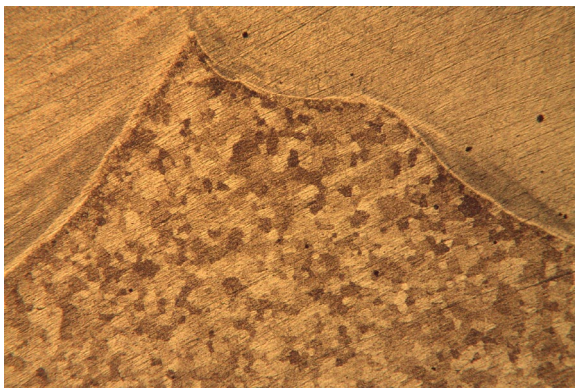

(i) Microstructure of ER90 HT bottom x5

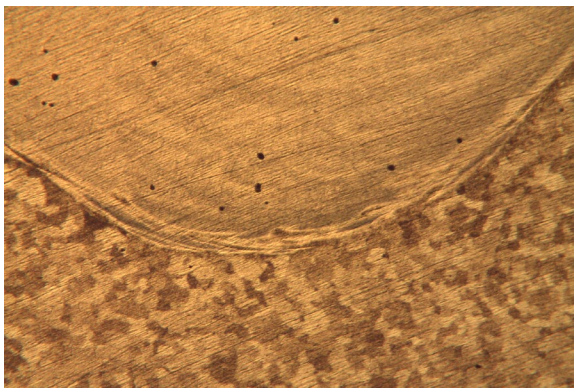

(ii) Microstructure of ER90 HT bottom x5

Figure 17: Micrographs of Low Alloy ER90 HT Bottom Sample**.**

5. CONCLUSIONS

The corrosion behaviour of high strength low alloy WAAM built and wrought steel were investigated in artificial seawater (3.5% NaCl) in deaerated and aerated conditions, at room and elevated temperatures.

- Initial studies show that the corrosion rate of wrought and WAAM built 2.4Cr 1 Mo steels are almost similar in both LPR and mass loss techniques at room temperature, but differ in aerated medium, at elevated temperature where the ER90 WAAM built structure shows improved corrosion resistance.

- Alloying compositions (Cr and Mo) improved the corrosion resistance, oxidation resistance, and hardenability thereby forming a uniformly dispersed carbide of very fine particles within the low alloy steels.
- Optical micrographs and hardness measurements confirm a martensitic structure in as deposited ER90, and a tempered-martensitic structure in heat-treated ER90 and wrought alloy steels.
- The micrographs show distinct pattern of corrosion near the substrate. This could be due the presence of a substrate S375 indicated by hardness measurements. Removal of substrate if different to the WAAM deposited material would reduce the likelihood of galvanic corrosion.
- It can be concluded that oil and gas industries need the right steel to ensure strong and long-lasting equipment, and WAAM route low alloy steels showed an improved hardness and corrosion resistance when compared with the wrought low alloy.

REFERENCES

American Society for Testing and Materials (ASTM), (1999). Standard Practice for Preparing, Cleaning, and Evaluating Corrosion Test Specimens. pp. 15-21.

Callister, Jr. W. D. (2007). *Materials Science and Engineering*: *An introduction*, 7th Edition, Department of Metallurgical Engineering, the University of Utah. John Wiley and Sons, Inc. pp. 1-739.

Callister, W. D. and Rethwisch, D. G. (2011). *Material Science and Engineering*, 8th edition, Asia: John Wiley and Sons.

Frankel, G. S. (2008). Electrochemical Techniques in Corrosion: Status, Limitations, and Needs. *Journal of American Society for Testing and Materials International*, **5(2)**: 3-64, DOI: 10.1520/JAI101241.

Goyal, M., Kumar, S., Bahadur, I., Verma, C. and Ebenso, E. E. (2018). Organic Corrosion Inhibitors for Industrial Cleaning of Ferrous and Non-Ferrous Metals in Acidic Solutions: A Review. *Journal of Molecular Liquids*, **256**: 565-573.

John, A. S. (2013). *Applications of Molybdenum Metal and Its Alloys*. 2nd edition, Published by the International Molybdenum Association (IMOA), London, UK.

Liu, Z., Gao, X., Du, L., Li, J., Wang, X. and Zhou, X. (2019). Corrosion Behaviour of Low-Alloy Steel Used for Flexible Pipes Exposed to a Seawater Environment. *Materials and Technology*, **53(1)**: 123-131, DOI: 10.17222/mit.2018.051.

Liu, Z., Gao, X., Du, L., Li, J., Wang, X. and Zhou, X. (2019). Corrosion Behaviour of Low-Alloy Steel Used for Flexible Pipes Exposed to a Seawater Environment. *Materials and Technology*, **53(1)**: 123-131, DOI: 10.17222/mit.2018.051.

Lyon, S. (2010). Corrosion of Carbon and Low Alloy Steels. *Shreir's Corrosion*, **3**: 1693-1736, DOI: 1016/B978-044452787-5.00190-6.

Masteel UK Limited (2017). Chrome Moly Steel: Features, Specifications, and Applications. 6, Three Spires

House, Station Road, Lichfield WS 13 6HX. https://masteel.co.uk/news/chrome-moly-steel-features-spec-applications/

National Association of Corrosion Engineers (NACE), (2017). Standard Guide for Laboratory Immersion Corrosion Testing of Metals. pp 1-10.

Rathi, M. G. and Jakhade, N. A. (2014). An Overview of Forging Processes with Their Defects. *International Journal of Scientific and Research Publications*, **4(6)**: 1-7.

Verma, C., Ebenso, E. E. and Quraishi, M. A. (2017). Ionic Liquids as Green and Sustainable Corrosion Inhibitors for Metals and Alloys: An Overview. *Journal of Molecular Liquids*, **233**: 403-414, DOI: 10.1016/j.molliq.2017.02.111.

Verma, C., Quraishi, M. A. and Singh, A. (2016). A Thermodynamical, Electrochemical, Theoretical and Surface Investigation of Diheteroaryl Thioesters as Effective Corrosion Inhibitors for Mild Steel in 1 M HCl. *Journal of the Taiwan Institute of Chemical Engineers*, **58**: 127-140, DOI: 10.1016/j.jtice.2015.06.020.

Wan Nik, W. B., Zulkifli, F., Rahman, M. M. and Rosliza, R. (2011). Corrosion Behaviour of Mild Steel in Seawater from Two Different Sites of Kuala Terengganu Coastal Area. *International Journal of Basic and Applied Sciences*, **11(06)**: 75-80, DOI: 114405-06-7676 IJBAS-IJENS.

Williams, S. W., Martina, F., Addison, A. C., Ding, J., Pardal, G. and Colegrove, P. (2016). Wire + Arc Additive Manufacturing. *Journal of Materials Science and Technology*, **32(7)**: 641-647, DOI: 10.1179/1743284715Y.0000000073.

Xu, X., Ganguly, S., Dinga, J., Guob, S., Williams, S. and Martina, F. 2018. Microstructural evolution and mechanical properties of maraging steel produced by wire +arc additive manufacture process. *Materials Characterization*, **1(43)**: 152-162.

Zima, G. E. (1977). *A Corrosion Critique of the 2.25Cr-1Mo Steel for LMFBR Steam Generation System Applications.* National Technical Information Service, Springfield, Virginia 22161, USA

https://dspace.org/

Corrosion behaviour of wire plus arc additive manufacturing (WAAM) built high strength pipeline steels

Shehu, Najib Usman; Impey, Susan A.; Ganguly, Supriyo

2022-03-01

https://doi.org/10.48419/IMIST.PRSM/rhazes-v14.31153

Shehu NU, Impey S, Ganguly S. (2022) Corrosion behaviour of wire plus arc additive manufacturing (WAAM) built high strength pipeline steels. RHAZES: Green and Applied Chemistry, Volume 14, pp. 95-115

Downloaded from a DSpace repository. https://dspace.org/